Transverse stability of the one-dimensional kink solution of the discrete Cahn-Hilliard equation

David Bettinson and George Rowlands
Department of Physics, University of Warwick, Coventry CV4 7AL, England
(Received 27 May 1997)

We give an analysis of a discrete version of the Cahn-Hilliard equation, which admits a one-dimensional kink solution. The stability of such a kink solution to perpendicular perturbations is analyzed using an asymptotic matching method as used by Bettinson and Rowlands [Phys. Rev. E **54**, 6102 (1996)] and a Green's function technique similar to that used by Shinozaki and Oono [Phys. Rev. E **47**, 804 (1993)]. The kink is found to be stable in both cases, but we find that the two methods do not agree, at first order in the growth rate, for perturbations of wave number close to $k=2p\pi$ (where p is some integer). Reasons for this disagreement and why the method given by Bettinson and Rowlands leads to the correct result are given. We then use equations derived in by Bettinson and Rowlands to compare stability results to those obtained for the continuous version of the equation. We also analyze the stability to perturbations of wave number close to $k=(2p+1)\pi$ and finally, using a Padé approximant, we give an expression for the growth rate of perturbations of all wavelengths. Our results quantify the difference between the continuum and discrete cases. [S1063-651X(98)02901-8]

PACS number(s): 64.60.−i, 02.90.+p, 02.30.Mv

I. INTRODUCTION

The continuous Cahn-Hilliard equation [1] has been used extensively to describe pattern formation resulting from a phase transition. Such decomposition has been observed in two-component systems such as alloys and glasses, where the phase transition is induced by rapidly quenching the system to below some critical temperature. For more physical background, derivation, and discussion see [2–4]. In [3] it is shown that to describe certain systems the wavelength of the decomposition is at the nanometer scale. This is too small for the continuum approximations of the Cahn-Hilliard equation to apply and it is shown that this approach fails to describe the kinetics of the experimentally observed decomposition. We use this as motivation for studying a discrete version of the Cahn-Hilliard equation, which we write in the form

$$\frac{\partial u_{n,m}}{\partial t}=\nabla^2\left[\frac{dF}{du}(u_{n,m})-\nabla^2 u_{n,m}\right], \tag{1}$$

where $u_{n,m}$ is the concentration parameter at the (n,m)th point of a two-dimensional lattice, and

$$\nabla^2 u_{n,m}=[u_{n+1,m}+u_{n-1,m}-2u_{n,m}]+q^2[u_{n,m+1}+u_{n,m-1}-2u_{n,m}], \tag{2}$$

where q is an anisotropy factor. We are interested in general perturbations that are perpendicular to the n direction, but a simple rotation of the perpendicular axes will turn such a problem into one that can be performed on a two-dimensional lattice. Equations such as Eq. (1) arise naturally in solid-state physics where the lattice is the atomic lattice. In [5], Eq. (1) was derived and analyzed for the early-time behavior described by linear perturbations to the homogeneous solution. The homogeneous solution was shown to be unstable. Of course nonlinear effects will introduce some form of saturation mechanism to this instability and, by analogy with many quite diverse systems in physics, chemistry, and biology (see, for example, [6] and references therein), will lead to a regular spatial pattern formation. We conjecture that this pattern can be described by an array of kink-type solutions. Thus in this paper, as a first step in a study of the possible existence of kink-type solutions, we study their linear stability.

We first look for one-dimensional stationary solutions to Eq. (1) and thus require solutions to

$$\Delta\overline{u_n}-F'(\overline{u_n})=0, \tag{3}$$

where $\Delta u_n=u_{n+1}+u_{n-1}-2u_n$. Unfortunately, unlike the analogous continuous problem, there are no general methods, such as phase plane analysis, to show the existence of periodic or kinklike solutions. We use a potential that is known to admit a stationary kink solution (see [7]), namely

$$F(u)=1-\frac{\alpha}{2}-u^2-\frac{\alpha}{2}\ln\left(\frac{2}{\alpha}(1-u^2)\right), \tag{4}$$

where α is some constant. This function has the advantage that it imposes the restriction $1\geqslant u\geqslant -1$, whereas if $F=(1-u^2)^2/4$, a commonly used form of the potential in studies of the Cahn-Hilliard equation, there is no such restriction. This latter case is unphysical because u is the percentage concentration of one of the two components and hence $|u|\leqslant 1$. It is shown in [7] that Eq. (3), along with the potential given by Eq. (4), admits a kink solution of the form

$$\overline{u_n}=\tanh\beta\tanh(n\beta+s), \tag{5}$$

where $\alpha=2\ \text{sech}^2\beta$ and s is an arbitrary phase. This potential F is plotted in Fig. 1. The exact form of F depends on the value of α taken, but we note that the two minima are always at $u=\pm\tanh\beta=\pm\sqrt{1-\alpha/2}$.

1063-651X/98/57(1)/169(10)/$15.00

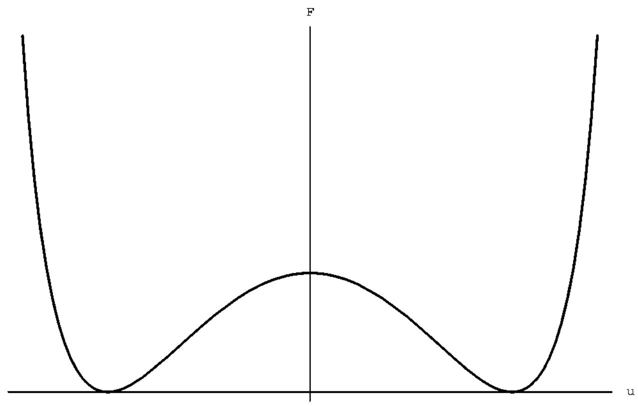

FIG. 1. Form of the potential $F(u)$.

A. Discrete to continuous equation

In this subsection we consider differences between the continuous and discrete kink. The continuous Cahn-Hilliard equation can be obtained from Eq. (1) in the limit as the variation of $u_{n,m}$ with n and m is slow compared to the underlying lattice spacing and is obtained by replacing the operator ∇^2 in Eq. (2) by $\partial^2/\partial x^2 + q^2\partial^2/\partial y^2$. To look for stationary, one-dimensional solutions we must solve

$$\left(\frac{d\overline{u}}{dx}\right)^2 = 2-\alpha-2\overline{u^2}-\alpha\ln\left(\frac{2}{\alpha}(1-\overline{u^2})\right). \tag{6}$$

We were unable to integrate this analytically, and so it has been solved numerically. The numerical solution is then compared to the analytical solution in the discrete case [given by Eq. (5) with $s=0$ and $n=x$]. The maximum error is found to be when $x=0$, which is confirmed if we consider Fig. 2. The maximum error is when $\overline{u}=0$, which since we are concerned with the kink solution, is when $x=0$. The maximum error in the approximate solution is plotted, for various values of β, in Fig. 3. For larger β, as $x\rightarrow\pm\infty$, the value of $\overline{u}(x)$ becomes closer to ± 1 and the kink becomes taller and steeper. This change in the shape of the stationary kink solution coincides with an increase in the error between the approximate (discrete) solution and the solution of Eq. (6). Thus, in conclusion, we see that the discrete and continuous forms are in good agreement for sufficiently small β.

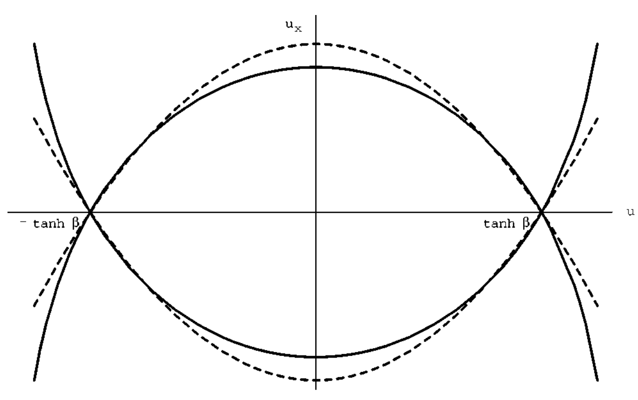

FIG. 2. Phase plane contours. Solid line, the continuous case, Eq. (6); dashed line, the approximate solution given by Eq. (5).

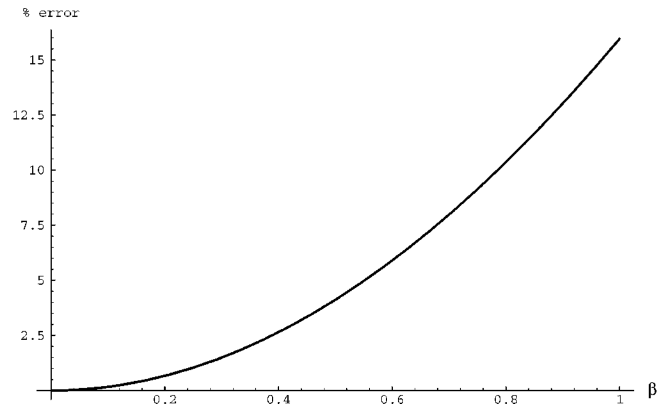

FIG. 3. Error between the approximate solution and the numerically calculated solution to Eq. (6), for various values of β.

B. Perturbing the kink solution

The remainder of this paper is devoted to asking whether such kink solutions can be observed in practice. To be observable it is necessary that small perturbations to the kink decay in time. To perturb a kink solution we write $u_{n,m} = \overline{u}_n + \delta u_{n,m}e^{\gamma t}$ and substitute this into Eq. (1). Neglecting products of $\delta u_{n,m}$, we obtain

$$\gamma\delta u_{n,m} = \nabla^2\left[\frac{d^2F}{du^2}(\overline{u}_n) - \nabla^2\right]\delta u_{n,m}. \tag{7}$$

Making use of the fact that the coefficients of $\delta u_{n,m}$ in Eq. (7) are independent of m we may write $\delta u_{n,m} = \phi_n e^{ikm}$ and then ϕ_n satisfies

$$-\gamma\phi_n = (\Delta - a^2)[\Delta - a^2 - F''(\overline{u}_n)]\phi_n, \tag{8}$$

with $a = 2q\sin(k/2)$ [in a truly three-dimensional problem we have $a^2 = 4q_1^2\sin^2(k_1/2) + 4q_2^2\sin^2(k_2/2)$, where q_1 and q_2 are the anisotropy factors and k_1, k_2 the wave numbers in the transverse directions].

Note that if we differentiate Eq. (3) with respect to the phase s we obtain

$$L\frac{\partial\overline{u}_n}{\partial s} = 0, \tag{9}$$

where $L = \Delta - F''(\overline{u}_n)$. Comparing this with Eq. (8) shows that a solution $\phi_n = \partial\overline{u}_n/\partial s$ exists when $a=0$ (i.e., $k = 2\pi p$) and $\gamma = 0$, that is, a marginally stable solution. In the continuous case, this marginally stable mode arises directly from the spatial invariance of the governing equation. In the discrete case the time-independent solution $\overline{u}_n$ is arbitrary up to a phase factor and the requirement of spatial invariance is replaced by one of phase invariance. In the next two sections we introduce two distinct methods to study the solutions of Eq. (8) and in particular the variation of the growth rate γ with a^2.

II. ASYMPTOTIC MATCHING METHOD

To solve the discrete linear equation (8) we extend a method, introduced in [8] and discussed in detail by Bettinson and Rowlands (BR) in Ref. [2]. The method is based on the fact that the correct asymptotic behavior of a solution to Eq. (8) must satisfy the form of this equation in the limit $|n|\to\infty$. In this limit the equation has constant coefficients and so is easily solvable. Thus we begin by considering the linear equation in the limit as $n\to\infty$. To do this we must know the asymptotic behavior of F''. From Eq. (4), it can be shown that if we ignore all exponentially decaying terms,

$$\lim_{n\to\infty}\frac{d^2F}{du_n^2}(\overline{u_n})=-4+\frac{8}{\alpha}=4\sinh^2\beta=K. \qquad (10)$$

Thus, in this same limit, Eq. (8) becomes

$$[(\Delta-a^2)^2-K(\Delta-a^2)+\gamma]\overline{\phi_n}=0, \qquad (11)$$

where $\overline{\phi_n}=\lim_{n\to\infty}\phi_n$. We assume solutions of the form $\overline{\phi_n}=e^{\lambda n}$ and find that

$$(e^{\lambda}+e^{-\lambda}-2-a^2)=\frac{1}{2}(K\pm\sqrt{K^2-4\gamma}). \qquad (12)$$

For a and γ small and for the positive square root in Eq. (12), the asymptotic form of the eigenfunction decays on a fast scale, that is $\overline{\phi_n}\sim e^{-2\beta n}$, while with the negative square root we find a slow variation that can be represented as a polynomial in n. Thus, for the slow variation we have

$$e^{\lambda}=1-a+a^2\left(\frac{1}{2}-\frac{\gamma_3}{2K}\right)+O(a^3) \qquad (13)$$

and

$$\overline{\phi_n}=Ae^{n\lambda}=A\left[1-na+a^2\left(\frac{n^2}{2}-\frac{n\gamma_3}{2K}\right)+O(a^3)\right], \qquad (14)$$

which is equivalent to Eq. (A4) in [2]. In Eq. (14), A is an arbitrary normalization constant and we have taken $\gamma=a^3\gamma_3$ since, as we show below, this is the form for small a.

The basis of BR's method is to remove any fast growing terms using a consistency condition and then to match the solution with the asymptotic form given by Eq. (14). To do this we consider the linear equation (8) for small a, by expanding the variables in a, namely,

$$\gamma=\gamma_1 a+\gamma_2 a^2+\gamma_3 a^3+\cdots,$$

$$\phi_n=\mathrm{sech}^2(n\beta)+\phi_{n,1}a+\phi_{n,2}a^2+\cdots. \qquad (15)$$

To first order in a, Eq. (8) is

$$\Delta L\phi_{n,1}=-\gamma_1\phi_{n,0}. \qquad (16)$$

Let $L\phi_{n,1}=\chi_n$ and note that since $\phi_{n,0}$ is symmetric about $n=0$ and Δ is a symmetry preserving operator, then χ_n is symmetric about $n=0$. Thus we write Eq. (16) as

$$-\gamma_1\phi_{n,0}=\Delta\chi_n=\chi_{n+1}+\chi_{n-1}-2\chi_n=P_{n+1}-P_n, \qquad (17)$$

where $P_{n+1}=\chi_{n+1}-\chi_n$. This equation is readily solved by iteration to give

$$P_{n+1}=P_0-\gamma_1\sum_{j=0}^{n}\phi_{j,0}, \qquad (18)$$

where P_0 is an arbitrary constant. Similarly,

$$\chi_{n+1}=\chi_n+P_0-\gamma_1\sum_{j=0}^{n}\phi_{j,0}$$
$$=\chi_0+(n+1)P_0-\gamma_1\sum_{l=0}^{n}\sum_{j=0}^{l}\phi_{j,0}$$
$$=\chi_0+(n+1)P_0-\gamma_1\sum_{j=0}^{n}(n+1-j)\phi_{j,0}, \qquad (19)$$

which is true for $n\geqslant 0$. Now we know that $P_{n+1}=\chi_{n+1}-\chi_n$ and so

$$P_1=\chi_1-\chi_0,$$
$$P_0=\chi_0-\chi_{-1}. \qquad (20)$$

Since χ_n is symmetric about $n=0$, this last result gives $P_0=-P_1$. Thus, from Eq. (18) we see that

$$P_0=\frac{\gamma_1}{2}. \qquad (21)$$

Using this result and Eq. (19) we find that

$$L\phi_{n,1}=\chi_n=c_1+\frac{n\gamma_1}{2}-\gamma_1\sum_{j=0}^{n-1}(n-j)\phi_{j,0} \qquad (22)$$

for $n\geqslant 1$ and

$$L\phi_{0,1}=\chi_0=c_1 \qquad (23)$$

for $n=0$ (note that we have replaced χ_0 by c_1).

In Appendix A, it is shown that the operator L is symmetric, and from this follows a consistency condition that when applied to Eq. (22) shows that $c_1=\hat{c}_1\gamma_1$, where $\hat{c}_1$ is some constant. Inserting this result into Eq. (22) gives

$$L\phi_{n,1}=\gamma_1\left[\hat{c}_1+\frac{n}{2}-\sum_{j=0}^{n-1}(n-j)\phi_{j,0}\right]. \qquad (24)$$

Using the asymptotic form as given by Eq. (14), since $\overline{\phi_{n,0}}=0$, then $\overline{\phi_{n,1}}$ must at most be a constant. To satisfy this condition we must have $\gamma_1=0$, leaving

$$L\phi_{n,1}=0, \qquad (25)$$

which implies that $\phi_{n,1}=A_1\phi_{n,0}$, where A_1 is some constant.

To second order in a, Eq. (8) becomes

$$\Delta(L\phi_{n,2}-\phi_{n,0})=-\gamma_2\phi_{n,0}, \qquad (26)$$

and using the results obtained at first order we find that this simplifies to

$$L\phi_{n,2}=c_2+\phi_{n,0}+\frac{\gamma_2 n}{2}-\gamma_2\sum_{j=0}^{n-1}(n-j)\phi_{j,0} \tag{27}$$

for $n\geqslant 1$ and

$$L\phi_{0,2}=c_2+1 \tag{28}$$

for $n=0$. Using a similar argument to that used to deduce $\gamma_1=0$ shows that $\gamma_2=0$ and thus

$$L\phi_{n,2}=c_2+\phi_{n,0} \tag{29}$$

for all n. Applying the consistency condition to Eq. (29), we find that $c_2=-I_2/I_1$, where

$$I_1=\sum_{n=-\infty}^{\infty}\phi_{n,0},$$

$$I_2=\sum_{n=-\infty}^{\infty}\phi_{n,0}^2, \tag{30}$$

and so Eq. (29) becomes

$$L\phi_{n,2}=\phi_{n,0}-\frac{I_2}{I_1}. \tag{31}$$

As $n\rightarrow\infty$ it is found, using Eq. (31), that (neglecting exponentially decaying terms)

$$\overline{\phi_{n,2}}=\frac{I_2}{KI_1}, \tag{32}$$

which has the same form as Eq. (20) in [2]. To third order in a, Eq. (8) is

$$\Delta(L\phi_{n,3}-\phi_{n,1})=-\gamma_3\phi_{n,0}, \tag{33}$$

from which we find that

$$L\phi_{n,3}=c_3+\phi_{n,1}+\frac{\gamma_3|n|}{2}-\gamma_3\sum_{j=0}^{n-1}(n-j)\phi_{j,0} \tag{34}$$

for $n\geqslant 0$ and

$$L\phi_{0,3}=c_3+A_1 \tag{35}$$

for $n=0$. Note that in Eq. (34) we have an absolute value of n since, as we have already stated, χ (or here $L\phi_{n,3}-\phi_{n,1}$) is symmetric about $n=0$. Applying the consistency condition to this equation, we find that

$$c_3=\frac{\gamma_3(I_3-I_4)-A_1I_2}{I_1}, \tag{36}$$

where I_1,I_2 are given above and

$$I_3=2\sum_{n=1}^{\infty}\phi_{n,0}\sum_{j=0}^{n-1}(n-j)\phi_{j,0},$$

$$I_4=\sum_{n=1}^{\infty}n\phi_{n,0}. \tag{37}$$

Now as $n\rightarrow\infty$, we write Eq. (34) as

$$(\Delta-K)\overline{\phi_{n,3}}=c_3+\frac{\gamma_3 n}{2}-\gamma_3\sum_{j=0}^{\infty}n\phi_{j,0}+\gamma_3\sum_{j=0}^{\infty}j\phi_{j,0}$$

$$=c_3+\gamma_3I_4-\frac{\gamma_3I_1}{2}n. \tag{38}$$

Thus the asymptotic form of the solution to third order in a is given by

$$\overline{\phi_{n,3}}=-\frac{c_3}{K}-\frac{\gamma_3I_4}{K}+\frac{\gamma_3I_1}{2K}n, \tag{39}$$

which is equivalent to Eq. (25) in [2]. If we combine this result with that given by Eq. (32) we can write

$$\overline{\phi_n}\propto 1+\frac{\gamma_3I_1^2}{2I_2}na+O(a^2). \tag{40}$$

A comparison of this result with that given by Eq. (14) shows that

$$\gamma_3=-\frac{2I_2}{I_1^2}, \tag{41}$$

which is equivalent to Eq. (27) in [2]. For small β, it is shown in Appendix B that these sums are well approximated by their integrals, in which case $\gamma_3=-2\beta/3$. We show later, in this limit, how the value of γ_3 is the same for both the discrete and continuous cases.

To fourth order in a, Eq. (8) is

$$\Delta(L\phi_{n,4}-\phi_{n,2})=-\frac{I_2}{I_1}-(\gamma_4+A_1\gamma_3)\phi_{n,0}. \tag{42}$$

From this it can be shown that the equivalent result to Eq. (21) to first order is

$$P_0=\frac{I_2}{2I_1}+\frac{1}{2}(\gamma_4+A_1\gamma_3), \tag{43}$$

so Eq. (42) becomes

$$L\phi_{n,4}-\phi_{n,2}=\frac{|n|}{2}(\gamma_4+A_1\gamma_3)+c_4-(\gamma_4+A_1\gamma_3)\sum_{j=0}^{n-1}(n-j)\phi_{j,0}-\frac{I_2}{2I_1}n^2, \tag{44}$$

where we have used the relationship

$$\sum_{j=0}^{n}(j+1)=\left(\frac{n}{2}+1\right)(n+1). \tag{45}$$

Now as $n\rightarrow\infty$, Eq. (44) becomes

$$(\Delta - K)\overline{\phi_{n,4}} = \hat{c}_4 + (\gamma_4 + A_1\gamma_3)\left(\frac{1}{2} - \sum_{j=0}^{\infty} \phi_{j,0}\right)n - \frac{I_2}{2I_1}n^2$$

$$= \hat{c}_4 - (\gamma_4 + A_1\gamma_3)\frac{I_1}{2}n - \frac{I_2}{2I_1}n^2 \qquad (46)$$

and thus

$$\overline{\phi_{n,4}} = -\frac{\hat{c}_4}{K} + \frac{I_1}{2K}(\gamma_4 + A_1\gamma_3)n + \frac{I_2}{2I_1K}n^2, \qquad (47)$$

which is equivalent to Eq. (30) in [2]. We now combine Eqs. (32), (36), (39), (41), and (47) to give

$$\overline{\phi_n} \propto 1 - an + a^2\left(\frac{\gamma_4 I_1^2 n}{2I_2} + \frac{2I_3 n}{I_1^2} - \frac{2I_4 n}{I_1^2} + \frac{2I_4 n}{I_1} + \frac{n^2}{2}\right) + O(a^3), \qquad (48)$$

and comparing this to Eq. (14) we find that

$$\gamma_4 = -\frac{4I_2}{I_1^4}\left[I_3 - I_4 + I_1 I_4 - \frac{I_2}{2K}\right], \qquad (49)$$

which is equivalent to Eq. (36) in [2]. Thus we can now write

$$\gamma = -\frac{2I_2}{I_1^2}a^3 - \frac{4I_2}{I_1^4}\left[I_3 - I_4 + I_1 I_4 - \frac{I_2}{2K}\right]a^4 + O(a^5) \qquad (50)$$

for small a.

We can now compare the results obtained for the discrete case to those obtained for the continuous Cahn-Hilliard equation. The difference between the discrete and continuous equations, both given by Eq. (1), is purely within the operator ∇^2. For the discrete equation ∇^2 is as defined in Eq. (2) of the present paper and for the continuous case it is taken to be the Laplacian operator. For the continuous case we use Eq. (27) and Eq. (36) of [2] where the stability is analyzed for a general potential. Using these equations with the potential F given by Eq. (4) and $a = k$, it is shown that

$$\gamma_3 = -\frac{\hat{I}_2}{2-\alpha},$$

$$\gamma_4 = -1 - \frac{\hat{I}_1\hat{I}_2}{(2-\alpha)^2} + \frac{\alpha\hat{I}_2^2}{8(2-\alpha)^3} + \frac{\hat{I}_2\hat{I}_3}{(2-\alpha)}, \qquad (51)$$

where the $\hat{I}_i$'s are definite integrals given by

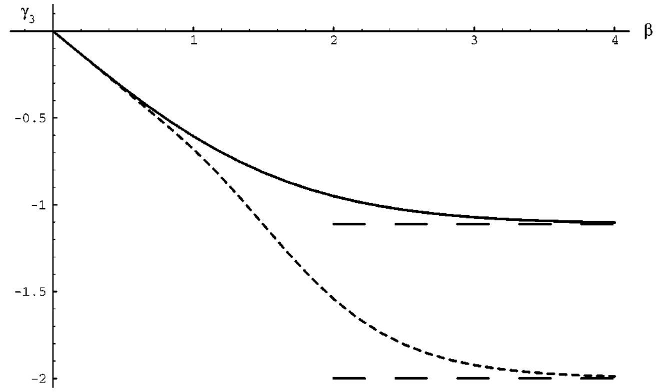

FIG. 4. Growth rate variable γ_3 as a function of β. Solid line, continuous equation (51); short-dashed line, discrete equation (41).

$$\hat{I}_1 = 2\int_0^{\sqrt{1-\alpha/2}} \left[\frac{u_0\left(\sqrt{1-\frac{\alpha}{2}} - u_0\right)}{\sqrt{2F(u_0)}}\right] du_0,$$

$$\hat{I}_2 = \int_{-\sqrt{1-\alpha/2}}^{\sqrt{1-\alpha/2}} \sqrt{2F(u_0)}\, du_0,$$

$$\hat{I}_3 = \frac{1}{K\sqrt{2-\alpha}}\int_0^{\sqrt{1-\alpha/2}} \left[\frac{Ku_0 - \sqrt{1-\frac{\alpha}{2}}F''(u_0)}{\sqrt{F(u_0)}}\right] du_0. \qquad (52)$$

These integrals, along with the results from the discrete analysis, are evaluated numerically for a range of β, and plotted in Fig. 4, and those lines labeled with an a in Fig. 5. These figures are the main results of our work as they show the similarities and differences between the solution of the continuous and discrete versions of the Cahn-Hilliard equation.

The expressions given for γ_3 in the discrete regime [Eq. (41)] and that in the continuous case [Eq. (51)] are easily analyzed for $\beta \to \infty$. It can be shown that

$$\lim_{\beta\to\infty} I_1 = \lim_{\beta\to\infty} I_2 = 1 \qquad (53)$$

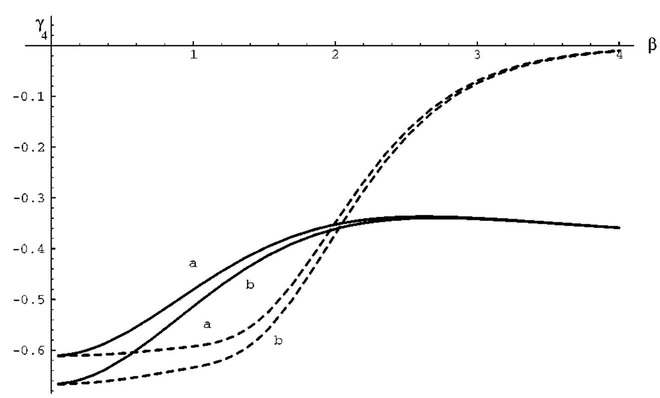

FIG. 5. Growth rate variable γ_4 against β. a, result obtained using the asymptotic matching method; b, result obtained using the Green's-function method. Solid line, continuous equation; dashed line, discrete equation.

and so in the discrete case

$$\lim_{\beta\to\infty} \gamma_3 = -2. \tag{54}$$

For the continuous case it can be shown that

$$\lim_{\beta\to\infty} \hat{I}_2 = \frac{\pi}{\sqrt{2}} \tag{55}$$

and so

$$\lim_{\beta\to\infty} \gamma_3 = -\frac{\pi}{2\sqrt{2}} \simeq -1.11. \tag{56}$$

These asymptotic forms are shown as long-dashed lines in Fig. 4.

This behavior is somewhat different from the time evolution of the unstable homogeneous solution $\overline{u}_n = 0$. Equation (7) still describes the time evolution, but now with $d^2F(\overline{u}_n)/du^2 = -2\tanh^2\beta$, from which it is simple to show that

$$\gamma = a^2(2\tanh^2\beta - a^2), \tag{57}$$

where $a = 2\sin(k/2)$ for the discrete equation and $a = k$ for the continuous equation. Thus, for small k the relationship between γ and the parameter β is the same for both the discrete and continuous equations. This is different from the decay rates of small-k perturbations to the kink solution as shown in Fig. 4. There we see that the decay rates differ from the discrete and continuous versions of the equation. We suggest that, for finite values of β, this decay rate difference is due the kink solution to the discrete equation being different to the kink solution in the continuous case, whereas the homogeneous solution is the same in both cases.

III. GREEN'S-FUNCTION METHOD

In Sec. II a method was developed to solve the eigenvalue equation (8) and give γ as a power series in a. It would be advantageous if a simpler method were available. The Green's-function method, introduced by Shinozaki and Oono in [9] to study the continuous case, is in fact simpler than the method of BR. In this section we apply this method to the discrete case and show that it gives an identical value for γ_3, but as in the continuous case, it gives an incorrect value for γ_4.

As in [9], we look for solutions to Eq. (8) for small a (i.e., $k \approx 2\pi p$). Formally, we introduce the Green's function for $\Delta - a^2$ and rewrite Eq. (8) in the form

$$(L - a^2)\phi_n = -\gamma \sum_{n'=-\infty}^{\infty} G(n;n')\phi_{n'}. \tag{58}$$

In Appendix C we show that the Green's function for $\Delta - a^2$ can, for small a, be written in the form

$$G(n;n') = -\frac{1}{2a} + \frac{|n-n'|}{2} + a\left(\frac{1}{16} - \frac{(n-n')^2}{4}\right) + O(a^2). \tag{59}$$

Using this, Eq. (58) becomes

$$(L - a^2)\phi_n = \frac{\gamma}{2a}\sum_{n'=-\infty}^{\infty} \phi_{n'} - \frac{\gamma}{2}\sum_{n'=-\infty}^{\infty} |n-n'|\phi_{n'} - a\gamma \sum_{n'=-\infty}^{\infty}\left(\frac{1}{16} - \frac{(n-n')^2}{4}\right)\phi_{n'}. \tag{60}$$

We perform a small-a expansion upon the variables, as in Eq. (15), and to zeroth order in a, Eq. (60) becomes

$$\frac{\gamma_1}{2}\sum_{n'=-\infty}^{\infty} \phi_{n',0} = L\phi_{n,0} = 0 \tag{61}$$

and so $\gamma_1 = 0$. To first order in a, Eq. (60) becomes

$$\frac{\gamma_2}{2}\sum_{n'=-\infty}^{\infty} \phi_{n',0} = L\phi_{n,1}. \tag{62}$$

Using the consistency condition as developed in Appendix A, we find that $\gamma_2 = 0$, which implies that Eq. (62) is now $L\phi_{n,1} = 0$, from which we find $\phi_{n,1} = A_1\phi_{n,0}$. To second order in a, Eq. (60) becomes

$$\frac{\gamma_3}{2}\sum_{n'=-\infty}^{\infty} \phi_{n',0} = L\phi_{n,2} - \phi_{n,0} \tag{63}$$

and now the consistency condition gives

$$\gamma_3 = -\frac{2I_2}{I_1^2}, \tag{64}$$

which is equivalent to Eq. (41) found using the asymptotic matching method. To third order in a, Eq. (60) becomes

$$\frac{1}{2}(A_1\gamma_3 + \gamma_4)I_1 - \frac{\gamma_3}{2}\sum_{n'=-\infty}^{\infty} |n-n'|\phi_{n',0} = L\phi_{n,3} - \phi_{n,1}. \tag{65}$$

In this case the consistency condition gives

$$\gamma_4 = -\frac{2I_2}{I_1^4}\sum_{n=-\infty}^{\infty} \phi_{n,0} \sum_{n'=-\infty}^{\infty} |n-n'|\phi_{n',0} \tag{66}$$

and using Eq. (D1) in Appendix D we see that

$$\gamma_4 = -\frac{4I_2}{I_1^4}(I_3 - I_4 + I_1 I_4). \tag{67}$$

A comparison of this equation to that given by Eq. (49) in Sec. II shows that here the potential F, through the terms involving K, has played no part in the value of γ_4. In [2], the continuous linear Cahn-Hilliard equation with a different potential was studied. The asymptotic method gave a value $\gamma_4 = -11/18$, whereas the Green's-function method gave $\gamma_4 = -2/3$. The 1/18 difference was again simply the contribution from the potential F. Thus we conclude that the Green's-function method gives the correct form for γ_3, but misses a contribution to γ_4 that depends explicitly on the detailed form of the potential.

We can now consider Figs. 4 and 5, where all results are shown. For γ_3, since both methods give the same answer, there are only two distinct curves (one for each of the continuous and discrete cases), whereas for γ_4 the Green's-function method always overestimates the decay rate and so there are four different curves. Note that for both γ_3 and γ_4, as $\beta \to 0$, the difference between the continuous and discrete answers tends to zero.

We have shown that the Green's function method is a quicker way to obtain stability results: γ_3 and γ_4 are obtained one order earlier than when using the asymptotic method. However, there is disagreement between the values of γ_4 given by each method. This we have shown is due to the potential affecting the asymptotic result, but not the Green's-function result at order a^4.

In [8] it is shown that to determine γ it is not sufficient just to remove exponentially secular terms as this leads to the wrong asymptotic form for the eigenfunction. It was shown that simply removing exponentially secular terms leads to the correct answer to lowest order, but breaks down at higher orders. Using the consistency condition, as in the Green's-function approach, actually removes exponentially secular terms and so will only give the correct value of γ to lowest order (i.e., γ_3). Thus we conclude that the method of using a Green's function together with a consistency condition to determine γ at anything other than lowest order is incorrect, from which we conclude that the results given by Eq. (67) above and (3.10) of [9] are wrong.

IV. NUMERICAL SOLUTION OF THE DISCRETE EQUATION

In this section we present results from numerical calculations of solutions to the discrete linear equation, namely, Eq. (8). These are performed using asymptotic knowledge of the solution to Eq. (11). It can be shown that the general bounded solution ϕ_n is such that

$$\lim_{n\to\infty} \phi_n = \overline{\phi_n} \propto \left[\frac{b_+}{2} - \frac{1}{2}\sqrt{b_+^2-4}\right]^n + c\left[\frac{b_-}{2} - \frac{1}{2}\sqrt{b_-^2-4}\right]^n, \tag{68}$$

where

$$b_\pm = \left[2 + a^2 + \frac{1}{2}(K \pm \sqrt{K^2 - 4\gamma})\right] \tag{69}$$

with the constant K given by Eq. (10). The relative amplitude of the two modes of decay in $\overline{\phi_n}$ is unknown and the constant c reflects this. Thus, for each value of a, at a particular value of β, we have two unknown quantities γ and c. A particular solution is found by choosing γ and c, using Eq. (68) as the solution for large n (we find that $n = 70$ is sufficient), and then iterating backward using Eq. (8).

We now note that in the analysis of Eq. (8) we have considered a symmetric eigenfunction. We develop a function to measure the symmetry of our numerically calculated eigenfunction. The absolute percentage error between ϕ_n and ϕ_{-n} is found for $1 \leqslant n \leqslant 30$, and these values are then summed. The final answer is used as a measure of the total error. We now vary γ and c in order to determine the minimum of this error function and thus find γ.

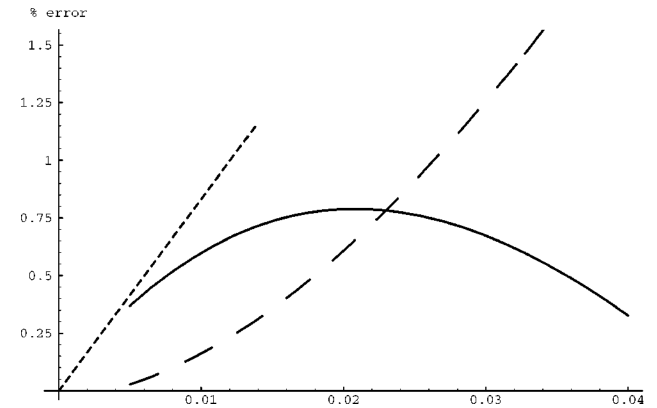

FIG. 6. Percentage error in the analytically calculated growth rates for $\beta = 0.1$ and various values of a. Long-dashed line, γ calculated using the asymptotic method; solid line, γ calculated using the Green's-function method; short-dashed line, $100(\gamma_{g,4} - \gamma_{a,4})a/\gamma_3$.

In Fig. 6 we show, for $\beta = 0.1$, the percentage error $100(\gamma - \gamma_a)/\gamma$, where γ_a is the value derived using our asymptotic method [given by Eq. (50)], and the percentage error $100(\gamma - \gamma_g)/\gamma$, where γ_g is the value derived using the Green's-function method [given by Eqs. (64) and (67)]. Clearly, as a gets larger, the absence of the a^5 term will influence our analytical results, *but* for small a, we see that γ_a is much closer to the numerically calculated value of γ. The short-dashed line is the percentage error of γ_g, calculated for small a, if we assume that $\gamma = \gamma_a$, namely, $100(\gamma_{g,4} - \gamma_{a,4})a/\gamma_3$. Clearly the two error curves for γ_g are in agreement, vindicating our assumption that $\gamma = \gamma_a$ for small a.

V. LARGE-*a* ANALYSIS

Now since $a = 2\sin(k/2)$, then $|a|$ has a maximum value of two when $k = \pi(1+2p)$, with p being any integer. Unlike the continuum case where a is just k and can take arbitrarily large values, here a is bounded. However, we assume a large-a expansion in analogy with the results given in [2]. Taking the dominant terms of Eq. (8), we find that

$$-\gamma\phi_n = a^4\phi_n, \tag{70}$$

which implies that to leading order $\gamma = -a^4$. As in Eqs. (44) and (45) of [2], we now scale the variables in $1/a$, thus

$$\phi_n = \phi_{n,a} + \frac{1}{a}\phi_{n,b} + \frac{1}{a^2}\phi_{n,c} + \cdots,$$

$$\gamma = -a^4 + \gamma_a a^3 + \gamma_b a^2 + \cdots. \tag{71}$$

To order a^3 we find that $\gamma_a = 0$. To order a^2 we find that

$$\left[\Delta - \frac{1}{2}[F''(\overline{u}_n) + \gamma_b]\right]\phi_{n,a} = 0 \tag{72}$$

is the equation to be solved. In principle this can be done to give γ_b, leaving

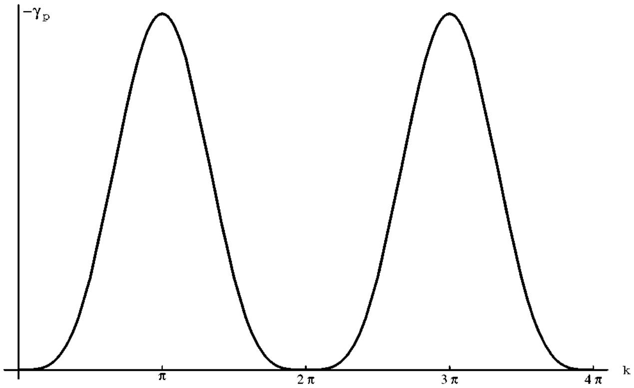

FIG. 7. Padé approximation to the growth rate given in Eq. (77).

$$\gamma = -a^4 + \gamma_b a^2 + \cdots. \tag{73}$$

Thus, to lowest order, for large a, $\gamma = -a^4$, and so if $a = 2$, to lowest order $\gamma = -16$. Also, since a is periodic in k we find that the growth rate of the kink solution is periodic, being marginally stable when $k = 2\pi p$ (p is some integer) and stable elsewhere.

VI. PADÉ APPROXIMATION TO THE GROWTH RATE

Since we now have approximations to the growth rate for small and large a, we use a Padé approximation for all a (as done in [2]). We assume the form of the growth rate to be given by

$$\gamma_p = \frac{b_0 a^3 (1 + b_1 a + b_2 a^2)}{1 + b_3 a}, \tag{74}$$

where the b_i are constants to be determined by our small- and large-a approximations to the growth rate. For small a we can write Eq. (74) as

$$\gamma_p = b_0 a^3 + b_0 (b_1 - b_3) a^4 + O(a^5). \tag{75}$$

Similarly, for large a we can write Eq. (74) as

$$\gamma_p = \frac{b_0 b_2}{b_3} a^4 + \frac{b_0}{b_3}\left(b_1 - \frac{b_2}{b_3} \right) a^3 + O(a^2). \tag{76}$$

A comparison of Eq. (75) to Eq. (50) and Eq. (76) to Eq. (73) will tell us the values of the b_i from which we can write Eq. (74) as

$$\gamma_p = \frac{a^3 \gamma_3^2}{[\gamma_3 - (1 + \gamma_4) a]} - a^4, \tag{77}$$

where $a = 2|\sin(k/2)|$. This form for γ_p is plotted in Fig. 7 as a function of k.

VII. CONCLUSIONS

There are three main points that arise from this paper. The first is related to the transverse stability of the discrete Cahn-Hilliard equation, the second relates to a flaw found when using a consistency condition, and finally we compare our findings with those of other authors who have considered the time evolution of discrete equations.

In this paper the transverse stability of a discrete equation is studied and it is shown that the discrete Cahn-Hilliard equation is, as with its continuous counterpart, stable to transverse perturbations. As the parameter $\beta \to 0$ the decay rate of perturbations decreases and the discrete answer converges to that obtained in the continuous case. For finite β the continuous case underestimates this decay rate. We have analyzed only one particular potential, but as found in [2], we expect the stability results to differ only quantitatively for different potentials. Importantly, the form for γ given by Eq. (50) is applicable for all potentials that admit kink solutions, with the detailed form of the kink only needed to evaluate the sums I_n. To lowest order, it is found that taller, steeper kink solutions are more stable.

In analyzing this equation, we have found important discrepancies in a commonly used method for determining the stability of fourth-order equations. The Green's-function method, as we have called it, appears to take no account of the particular potential and, as we have shown, gives an incorrect value to the first order correction to the decay rate for small a.

In [3] it was pointed out that the derivation of the discrete Cahn-Hilliard equation depends on a gradient expansion of the free energy. The approximation used rejects all high-order terms, thus limiting the validity of the equation to relatively smooth solutions. In [3] it is shown numerically, for three different models of phase separation (one of which is the continuous Cahn-Hilliard equation), that the system under consideration always evolved to the same final state but that the time scales of evolution were model dependent. Similarly, we have shown that differences between the discrete and continuous Cahn-Hilliard equations are only quantitative, namely, the kink solution is stable but the decay rate does differ between the two cases. This means that the total time for the evolution of an unstable homogeneous initial state to a kink or array of kinks differs depending on whether one uses the discrete or continuum model. The results given in this paper can be used to give estimates of the differences in this time.

ACKNOWLEDGMENT

This work was carried out while D.B. was supported by an EPSRC grant.

APPENDIX A: SYMMETRIC OPERATOR

Here we show that $L = \Delta - F''(\overline{u_n})$ is a symmetric operator. Consider the equation

$$I = \sum_{n=-\infty}^{\infty} \psi_n L \phi_n, \tag{A1}$$

where ψ_n is an arbitrary function that tends to zero as $n \to \pm\infty$. Then

$$I=\sum_{n=-\infty}^{\infty}\psi_n[\Delta-F''(\overline{u_n})]\phi_n$$
$$=\sum_{n=-\infty}^{\infty}\psi_n[\phi_{n+1}+\phi_{n-1}-2\phi_n-F''(\overline{u_n})\phi_n]$$
$$=\sum_{n=-\infty}^{\infty}\phi_n[\psi_{n+1}+\psi_{n-1}-2\psi_n-F''(\overline{u_n})\psi_n]$$
$$=\sum_{n=-\infty}^{\infty}\phi_n L\psi_n, \tag{A2}$$

so that

$$\sum_{n=-\infty}^{\infty}\psi_n L\phi_n=\sum_{n=-\infty}^{\infty}\phi_n L\psi_n \tag{A3}$$

for arbitrary ψ_n, which proves that L is symmetric. Using this result, we can obtain a consistency condition that bounded solutions exist for any equation of the form

$$L\phi_n=S_n. \tag{A4}$$

First multiply by $\phi_{n,0}$ and sum over all n. Now use the result that L is symmetric, $L\phi_{n,0}\equiv 0$, and the consistency condition

$$\sum_{n=-\infty}^{\infty}\phi_{n,0}\ S_n=0 \tag{A5}$$

follows.

APPENDIX B: EVALUATION OF CERTAIN INFINITE SUMMATIONS

The original series I_1 and I_2 [Eq. (30)] give convergent results for $\beta\to\infty$. Here we find a series representation appropriate for $\beta\to 0$. For this we use the Poisson sum formula (see [10], p. 466), which states that

$$\sum_{n=-\infty}^{\infty}f(\alpha n)=\frac{\sqrt{2\pi}}{\alpha}\sum_{m=-\infty}^{\infty}F\left(\frac{2m\pi}{\alpha}\right), \tag{B1}$$

where F is the Fourier transform of f,

$$F(k)=\frac{1}{\sqrt{2\pi}}\int_{-\infty}^{\infty}f(x)e^{ikx}dx. \tag{B2}$$

Now $I_1=\Sigma_{n=-\infty}^{\infty}\ \mathrm{sech}^2(n\beta)$ and so using Eq. (B1) we can say

$$I_1=\frac{\sqrt{2\pi}}{\beta}\sum_{m=-\infty}^{\infty}F\left(\frac{2m\pi}{\beta}\right), \tag{B3}$$

where

$$F(x)=\frac{1}{\sqrt{2\pi}}\int_{-\infty}^{\infty}\frac{\cos xt}{\cosh^2 t}dt. \tag{B4}$$

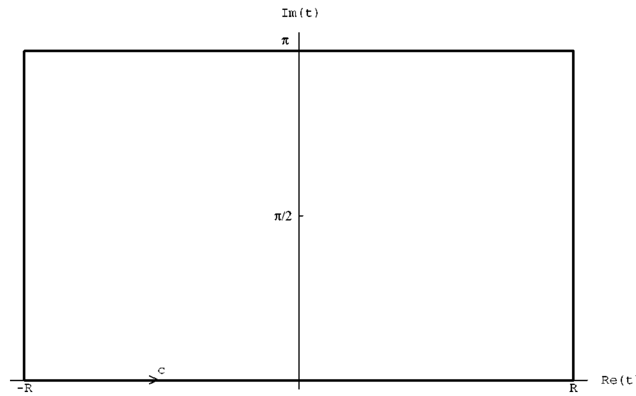

FIG. 8. Path of integration.

Note that the function $\cos xt/\cosh^2 t$ has poles when $t=i\pi(1+2p)/2$, where $p=0,1,2,\ldots$. To solve the integral we use complex integration. The contour chosen is that in Fig. 8. By Cauchy's theorem

$$\oint_c\frac{\cos xt}{\cosh^2 t}dt=2\pi i\sum\quad(\text{residues}). \tag{B5}$$

The residue of the function $\cos xt/\cosh^2 t$ about $i\pi/2$ is $ix\sinh(\pi x/2)$. Using Eq. (B5), we find that

$$\int_{-\infty}^{\infty}\frac{\cos xt}{\cosh^2 t}dt-\cosh\pi x\int_{-\infty}^{\infty}\frac{\cos xt}{\cosh^2 t}dt=2\pi i\left(ix\sinh\frac{\pi x}{2}\right), \tag{B6}$$

so that

$$\int_{-\infty}^{\infty}\frac{\cos xt}{\cosh^2 t}dt=\frac{\pi x}{\sinh\frac{\pi x}{2}} \tag{B7}$$

and thus

$$F\left(\frac{2m\pi}{\beta}\right)=\frac{m\sqrt{2\pi^3}}{\beta\sinh\frac{m\pi^2}{\beta}}. \tag{B8}$$

Combining this result with Eq. (B3), we find that

$$I_1=\frac{2\pi^2}{\beta^2}\sum_{m=-\infty}^{\infty}\frac{m}{\sinh\frac{m\pi^2}{\beta}}=\frac{2\pi^2}{\beta^2}\left[\frac{\beta}{\pi^2}+2\sum_{m=1}^{\infty}\frac{m}{\sinh\frac{m\pi^2}{\beta}}\right]. \tag{B9}$$

Now we expand Eq. (B9) for small β to give

$$I_1=\frac{2\pi^2}{\beta^2}\left[\frac{\beta}{\pi^2}+4e^{-\pi^2/\beta}(1+2e^{-\pi^2/\beta}+\cdots)\right], \tag{B10}$$

which we can approximate to

$$I_1=\frac{2}{\beta}+\frac{8\pi^2}{\beta^2}e^{-\pi^2/\beta}. \tag{B11}$$

Here we note that the first term is simply the integral limit of the sum. Also, for small β, the second term becomes insignificant compared to the first (for $\beta=1/\sqrt{2}$, the second term is 0.0048% of the first). Thus, for $\beta\leqslant 1$, the value of the sum is well approximated by the integral.

In a similar manner we find that

$$I_2=\frac{4\pi^2}{3\beta^2}\left[\frac{\beta}{\pi^2}+2\sum_{m=1}^{\infty}\frac{m(\beta^2+m^2\pi^2)}{\beta^2\sinh\frac{m\pi^2}{\beta}}\right], \tag{B12}$$

which for small β becomes

$$I_2=\frac{4}{3\beta}+\frac{16\pi^2}{3\beta^2}\left(1+\frac{\pi^2}{\beta^2}\right)e^{-\pi^2/\beta}. \tag{B13}$$

Again, as $\beta\to 0$, this sum over all n takes the same value as the integral over all space.

APPENDIX C: DISCRETE GREEN'S FUNCTION

Here we look for the Green's function for the discrete operator $\Delta-a^2$, where $\Delta\phi_n=\phi_{n+1}+\phi_{n-1}-2\phi_n$. Using

$$(\Delta-a^2)G(n;n')=G_{n+1}(n')+G_{n-1}(n')-(2+a^2)G_n(n') =\delta_{n,n'}, \tag{C1}$$

we look for solutions $G_n\propto e^{\lambda n}$, for $n\neq n'$. It is found that

$$e^{\lambda}=1+\frac{a^2}{2}\pm a\sqrt{1+\frac{a^2}{4}}. \tag{C2}$$

So since $G(n;n')$ must remain bounded as $n\to\pm\infty$, for $n>n'$,

$$G=G_+e^{\lambda_- n}, \tag{C3}$$

and for $n<n'$,

$$G=G_-e^{\lambda_+ n}, \tag{C4}$$

where

$$e^{\lambda_\pm}=1+\frac{a^2}{2}\pm a\sqrt{1+\frac{a^2}{4}} \tag{C5}$$

and G_+,G_- are both constants. Now Eqs. (C3) and (C4) must equate when $n=n'$ and so

$$G_+e^{\lambda_- n'}=G_-e^{\lambda_+ n'}. \tag{C6}$$

Also, if we sum Eq. (C1) from $n=n'-1$ to $n=n'+1$ we find that

$$G_+=\frac{e^{-\lambda_- n'}}{e^{\lambda_-}+e^{-\lambda_+}-2-a^2}. \tag{C7}$$

Thus, finally, we can say that for $n>n'$,

$$G=\frac{e^{\lambda_-(n-n')}}{e^{\lambda_-}+e^{-\lambda_+}-2-a^2}, \tag{C8}$$

and for $n<n'$,

$$G=\frac{e^{\lambda_+(n-n')}}{e^{\lambda_-}+e^{-\lambda_+}-2-a^2}. \tag{C9}$$

Since we are interested in small-a behavior, we expand Eqs. (C8) and (C9) and find for all n and small a

$$G(n;n')=-\frac{\left(1+\frac{a^2}{2}-a\sqrt{1+\frac{a^2}{4}}\right)^{|n-n'|}}{2a+\frac{a^3}{4}} =-\frac{1}{2a}+\frac{|n-n'|}{2}+a\left(\frac{1}{16}-\frac{(n-n')^2}{4}\right)+O(a^2). \tag{C10}$$

APPENDIX D: SUMMATION MANIPULATION

In Sec. III the value of γ_4 obtained by the Green's function method is given by Eq. (66). This can be extended as

$$\begin{aligned}\sum_{n=-\infty}^{\infty}\phi_n\sum_{j=-\infty}^{\infty}|n-j|\phi_j &=2\sum_{n=1}^{\infty}\phi_n\sum_{j=-\infty}^{\infty}|n-j|\phi_j+\sum_{j=-\infty}^{\infty}|j|\phi_j\\ &=2\left[\sum_{n=1}^{\infty}\phi_n\sum_{j=-\infty}^{n-1}(n-j)\phi_j-\sum_{n=1}^{\infty}\phi_n\sum_{j=n+1}^{\infty}(n-j)\phi_j\right]\\ &\quad+2I_4=2\left[I_3+3\sum_{n=1}^{\infty}n\phi_n\sum_{j=1}^{\infty}\phi_j-\sum_{n=1}^{\infty}n\phi_n\sum_{j=0}^{\infty}\phi_j\right]\\ &\quad+2I_4=2\left(I_3+2I_4\sum_{n=1}^{\infty}\phi_n\right)=2(I_3-I_4+I_1I_4).\end{aligned} \tag{D1}$$

[1] J. W. Cahn and J. E. Hilliard, J. Chem. Phys. **28**, 258 (1958).

[2] D. Bettinson and G. Rowlands, Phys. Rev. E **54**, 6102 (1996).

[3] J. M. Hyde, A. P. Sutton, J. R. G. Harris, A. Cerezo, and A. Gardiner, Modelling Simul. Mater. Sci. Eng. **4**, 33 (1996).

[4] A. Novick-Cohen and L. A. Segel, Physica D **10**, 277 (1984).

[5] H. E. Cook, D. de Fontaine, and J. E. Hilliard, Acta Metall. **17**, 765 (1969).

[6] *Modeling the Dynamics of Biological Systems*, edited by E. Mosekilde and O. G. Mouritsen (Springer-Verlag, Berlin, 1995).

[7] G. Rowlands, J. Phys. A **27**, 5313 (1994).

[8] M. A. Allen and G. Rowlands, J. Plasma Phys. **50**, 413 (1993).

[9] A. Shinozaki and Y. Oono, Phys. Rev. E **47**, 804 (1993).

[10] P. M. Morse and H. Feshbach, *Methods of Theoretical Physics* (McGraw-Hill, New York, 1953).